Drug Delivery and Translational Research (2023) 13:400–418
https://doi.org/10.1007/s13346-022-01219-1

REVIEW ARTICLE

Liquid antisolvent crystallization of pharmaceutical compounds: current status and future perspectives

Rahul Kumar[1] · Amit K. Thakur[1] · Nilanjana Banerjee[1] · Ashutosh Kumar[2] · Gajendra Kumar Gaurav[3] · Raj Kumar Arya[4]

Accepted: 30 July 2022 / Published online: 11 August 2022

Abstract

The present work reviews the liquid antisolvent crystallization (LASC) to prepare the nanoparticle of pharmaceutical compounds to enhance their solubility, dissolution rate, and bioavailability. The application of ultrasound and additives is discussed to prepare the particles with narrow size distribution. The use of ionic liquid as an alternative to conventional organic solvent is presented. Herbal compounds, also known for low aqueous solubility and limited clinical application, have been crystalized by LASC and discussed here. The particle characteristics such as particle size and particle size distribution are interpreted in terms of supersaturation, nucleation, and growth phenomena. To overcome the disadvantage of batch crystallization, the scientific literature on continuous flow reactors is also reviewed. LASC in a microfluidic device is emerging as a promising technique. The different design of the microfluidic device and their application in LASC are discussed. The combination of the LASC technique with traditional techniques such as high-pressure homogenization and spray drying is presented. A comparison of product characteristics prepared by LASC and the supercritical CO_2 antisolvent method is discussed to show that LASC is an attractive and inexpensive alternative for nanoparticle preparation. One of the major strengths of this paper is a discussion on less-explored applications of LASC in pharmaceutical research to attract the attention of future researchers.

Keywords Nanoparticle · Antisolvent · Crystallization · Microfluidic · Bioavailability

Introduction

The drugs having low aqueous solubility and high gastrointestinal permeability are classified as Class II under Biopharmaceutics Classification System (BCS) [1]. The low aqueous solubility of BCS II drugs leads to a slow dissolution rate and subsequently low bioavailability [2]. For example, eprosartan mesylate (EPM) has very low aqueous solubility, 80 µg/ml, and is reported to have 13% bioavailability after oral administration [3]. A higher dose of EPM, 600 mg/day, is required in pharmaceutical dosage form to achieve the required therapeutic effect [4]. If the solubility of Class II drugs is increased, these can be easily absorbed in the gastrointestinal tract after oral administration. This has attracted great interest among researchers to explore the strategies to improve the aqueous solubility of BCS II drugs. The different formulation strategies include nanosuspension, micro-emulsion, solid dispersion, a cyclo-dextrin inclusion complex, and a solid self-emulsifying drug delivery system (solid-SEDDS). The recent application of these strategies to improve the aqueous solubility, dissolution rate, and bioavailability of BCS II drugs/active pharmaceutical ingredients (APIs) is shown in Table 1.

Nanonization is one of the promising approaches to improve the solubility, dissolution rate, and bioavailability of poorly water-soluble drugs. The reduction in particle size

✉ Rahul Kumar
rahul.iitrahul@gmail.com; rahul.kumar@ddn.upes.ac.in

1 Department of Chemical Engineering, Energy Cluster, University of Petroleum and Energy Studies, Dehradun 248007, Uttarakhand, India

2 Department of Chemical Engineering, Indian Institute of Technology Delhi, 110016 New Delhi, India

3 Sustainable Process Integration Laboratory, SPIL, NETME Centre, Faculty of Mechanical Engineering, Brno University of Technology, VUT Brno, Technická 2896/2, 616 69 Brno, Czech Republic

4 Department of Chemical Engineering, Dr. B.R. Ambedkar National Institute of Technology, Jalandhar, India

Table 1 Formulation strategies of BCS II drugs

Technique	API	References
Solid dispersion	Sorafenib, fenofibrate, regorafenib, clarithromycin,	[5–8]
Micro-emulsion	Felodipine, Mebendazole, raloxifene, celecoxib, repaglinide	[9–13]
Inclusion Complexation	Dibenzalacetone, praziquantel, etodolac, baicalin	[14–17]
Solid-SEDDS	Carvedilol, Prasugrel Hydrochloride, aripiprazole, azithromycin	[18–21]
Nanonization	Cannabidiol, sertraline hydrochloride, Nintedanib, fluconazole	[22–25]

leads to a higher effective particle surface area for dissolution and subsequently higher dissolution rate, solubility, and bioavailability [26, 27]. The typical size of drug nanoparticles is in the range of 100–200 nm stabilized with surfactant or polymer or a combination of both [28]. Nanosuspension is also reported to reduce the fast/fed variability of anti-cancer molecules [29]. The advantage of nanosuspension is high drug loading, low side effects, low toxicity, and improved safety [30].

The techniques of nanonization of pharmaceutical compounds are broadly categorized into the top-down method and bottom-up methods. The top-down method involves a physical process of mechanical attrition to reduce large-size drug particles into fine particles in submicron ranges. The wet media milling and high-pressure homogenization (HPH) are the conventional top-down methods for the preparation of nanoparticles in pharmaceutical industries [31]. The bottom-up approach involves a physicochemical method in which an API is dissolved in a solution and then precipitated to generate nanoparticles. Supercritical carbon dioxide (SC CO2)-based crystallization [32, 33], liquid antisolvent crystallization [34], and pulsed laser ablation, etc., are some of the bottom-up approaches to preparing the nanoparticles [35]. A high energy requirement, mechanical stress, inconsistent crystal form in different batches, and product contamination are the main challenges associated with top-down methods. Researchers have explored the bottom-up methods to address these limitations of top-down methods.

The liquid antisolvent crystallization process is gaining importance due to its easy operation and mild conditions. LASC is also reported to least expensive method to prepare nanoparticles [36]. This method is suitable for APIs which are thermally sensitive or their solubility is a weak function of temperature [37]. In LASC, API is dissolved in a solvent to prepare a solution. This solution is mixed with another solvent having low solubility for the API and is known as antisolvent. The reduction in solubility of API in the binary mixture of solvent-antisolvent generates the supersaturation followed by nucleation and growth phenomena. The knowledge of the solubility of APIs in solvent and solvent-antisolvent mixture is indispensable to prepare the nanosuspension [38, 39]. The solubility of API in pure solvent and binary mixture can be measured experimentally by gravimetric method [40], spectroscopy [41–44], and laser method [45]. The experimental measurement of solubility is time-consuming and expensive [39, 46]. Several empirical and thermodynamic models such as the Wilson, NRTL, UNIQUAC, Yaws model, modified Apelblat model, λh model, Jouyban-Acree model, and Apelblat-Jouyban-Acree model, Sun et al. model, and Ma et al. model are employed by researchers to correlate and predict the solubility of APIs in pure solvent and binary mixture [47].

Liquid antisolvent crystallization leads to the formation of fine particles, micron- to nano-range, depending upon the process conditions. The process variables such as type of solvent, drug concentration, mixing rate, drug solution injection rate, and temperature affect supersaturation and subsequently nucleation and growth phenomena. The particle characteristics including particle size, particle size distribution, morphology, and crystalline/amorphous form depend upon supersaturation and can be controlled by tuning the process variables. LASC has also been found to change the polymorphic form of the drug [48]. The use of ultrasound and mixing in the microfluidic channel have been explored as process intensification of LASC. The polymers and surfactants known as additives are found to inhibit crystal growth, prevent the agglomeration of the precipitated particles, and stabilize the nanosuspension. In this work, these aspects related to LASC are critically reviewed and followed by a future perspective.

Liquid antisolvent crystallization: fundamentals and operation

Liquid antisolvent crystallization is carried out by mixing drug solution (drug + solvent) and antisolvent to create supersaturation. The product characteristics depend upon supersaturation which in turn is influenced by the mixing between solution and antisolvent. The mixing can be done in (1) semi-batch mode and (2) continuous mode. In semi-batch operation, drug solution is continuously injected into the vessel containing the antisolvent. A schematic diagram of LASC has been shown in Fig. 1 [49]. The magnetic stirrer or impeller is used to enhance the mixing between drug solution and antisolvent. The different pre-mixers such as Roughton or T-mixers have also been used to enhance the mixing [50].

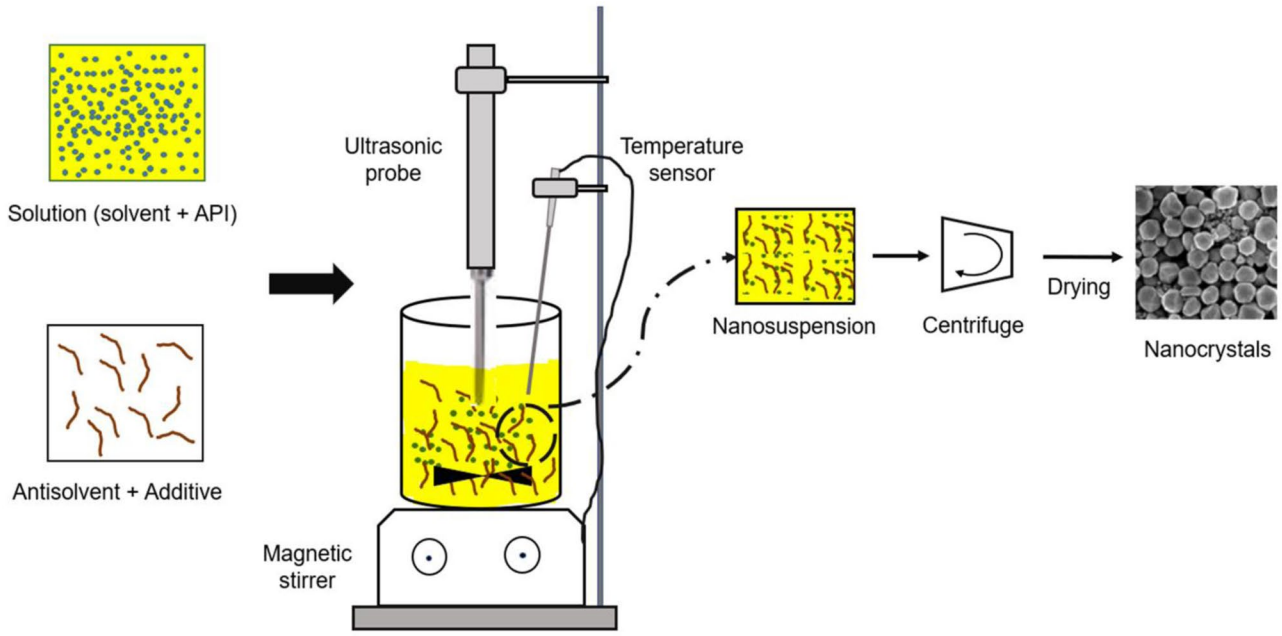

Fig. 1 Schematic of the liquid antisolvent crystallization technique

The first step to carry out the LASC is the screening of solvent for a particular API. The solubility of API varies in different solvents. The solvent with maximum drug loading is generally considered the suitable solvent for LASC [51]. Water is the most suitable antisolvent for BCS II drugs due to their low aqueous solubility. The solvent must be fully miscible with antisolvent to prevent the formation of an emulsion during the crystallization process [52]. The viscosity ratio of solvent and antisolvent is also a critical factor and its value must be less than 3 to prevent the formation of transient emulsion [53]. The nanosuspension can be converted to dry powder by centrifugation or filtration followed by drying using a vacuum oven or by freeze-drying/spray drying [54].

The use of ultrasound and static mixer in LAS crystallization reduces both the induction time and metastable zone width [55]. This enhances the mixing and consequently the secondary nucleation rate. Gandhi et al. [56] prepared the rapidly dissolving (orodispersible) tablet of nitrendipine nanocrystals. The nanosuspension of nitrendipine was prepared by antisolvent crystallization using ultrasound. The saturation solubility of nitrendipine was increased remarkably (26.14-fold) in comparison to raw nitrendipine. The in vitro dissolution of tablets formed by nanosuspension was found to be completed in 8 min as compared to 30 min for raw nitrendipine tablets. Lee et al. [57] studied the antisolvent crystallization of NaCl using sonication by the ultrasonic probe and high-frequency ultrasound. The authors reported that ultrasound-generated sodium chloride crystals have a more symmetrical cubic structure compared to crystals produced by a high shear mixer that produced asymmetric and irregular-shaped crystals.

Nano-suspension of the pure pharmaceutical compound is unstable which may be attributed to aggregation due to highly attractive inter-particle forces (van der Waals force, hydrophobic forces) and Ostwald ripening [58]. In Ostwald ripening, particle size increases with time due to the transport of materials from smaller particles to larger particles [59]. The polymer/surfactant (additive), known as stabilizers, are used in the stabilization of nanosuspension produced by LASC. The polymer and non-ionic surfactant provide steric hindrance while charged surfactant leads to electrostatic repulsion. The multivalent cations of a non-toxic metal are also explored to stabilize the nanosuspension [60]. Extensive screening is required to select the suitable stabilizer for a particular API nanosuspension as there is no universal stabilizer. The additive type and its concentration are crucial factors affecting the physical stability and in vivo performance of the nanosuspension [61]. The selection of additive is done by experimental investigation and then its concentration is optimized using design of experiment techniques [62, 63]. At lower or higher concentrations, larger particles are obtained in the LASC. This is attributed to the fact that at lower concentrations a complete monolayer at the surface of the particles may not be formed. At higher concentrations, agglomeration among particles increased due to attraction among colloidal particles leading to the formation of larger particles [64]. The use of additive is combined with ultrasound in LASC to control the product characteristics. The

solubility, flowability, and dissolution rate of pharmaceutical compounds are found to be morphology-dependent [65]. Rangaraj et al. [66] prepared the nanoparticle of ibrutinib using pluronic F-127 as a stabilizer under ultrasonic conditions. The average particle size and the polydispersity index were reported in the range of 278.6 to 453.2 nm and 0.055 to 0.198, respectively. The transformation from the crystalline to amorphous form was obtained which was found stable for 6 months at room temperature. The reduced fast/fed variability of a nano-suspension was observed when compared with the unprocessed drug. The LASC of API in the presence of a stabilizer is reported to modify the crystal habit and morphology [67, 68], and to enhance the dissolution rate [69, 70] and polymorphism control [71, 72]. In Table 2, the application of different stabilizers used in LAS crystallization is presented.

To carry out LASC, the API must have good solubility in the pharmaceutically acceptable solvent. However, the majority of the pipeline drugs have low solubility in an organic solvent which is typically used for crystallization [86]. Moreover, polar organic solvents are volatile, flammable, and toxic and cause concern in wastewater disposal mainly due to the difficulty faced in the recovery and re-usage steps [87]. The alternative to traditional volatile organic solvents are ionic liquids (ILs) which have been investigated in the LASC process as these exhibit sufficient solubility of drugs [88, 89].

ILs are defined as molten salts composed of large organic cations and organic/inorganic anions with a melting point below 100 °C. ILs are thermally and chemically stable, non-flammable, and exhibit strong solvation ability for a wide variety of compounds [90]. They are also referred to as "designer solvents" due to their flexibility in cation/anion selection [91]. They have a very wide range of applications in the pharmaceutical field such as synthesis, crystallization, liquid forms of API, improvement of drug solubility, and development of drug delivery systems. The interested readers may go through the reviews on the application of ILs in pharmaceutical research [92, 93]. The use of ILs as solvents in LASC is summarized in Table 3.

LASC has been explored to enhance solubility, dissolution rate, and bioavailability of herbal compounds. Although the herbal compounds have several pharmacological effects, their clinical application and therapeutic efficiency are limited due to poor aqueous solubility leading to low bioavailability. Sahibzada et al. [98] successfully prepared berberine nanoparticles using LASC and reported substantial improvement in the liver function test, enzyme levels, and liver histopathology in the animals treated with berberine nanoparticles in comparison to the unprocessed berberine. Gera et al. [99] prepared the nanoparticle of rutin, a herbal compound exhibiting a therapeutic benefit to osteoporosis patients. The average particle size of rutin nanoparticles was 122 nm at optimized conditions of LASC. The dissolution rate increased to 87% for rutin nanoparticles as compared to 39% for the pure drug in 60 min in phosphate media under similar conditions. Wu et al. [100] explored LASC to prepare the nanoparticles of honokiol, a traditional Chinese herbal medicine, of poor aqueous solubility exhibiting several pharmacological properties, such as anticancer effects, anti-inflammatory effects, and antianxiety effects. They reported that the dissolution rate of honokiol was 20.41-fold and 26.2-fold that of free honokiol in artificial gastric juice and artificial intestinal juice respectively. In Table 4, the application of LASC to prepare the nanoparticles of herbal compounds is presented.

The LASC process has also been explored to prepare the encapsulated nanoparticles [111]. Sun et al. [112] prepared dihydromyricetin (DMY) encapsulated zein-caseinate nanoparticles (DZP) which led to 1.95-fold enhancement of oral bioavailability of DMY. Dihydromyricetin and Zein, in the mass ratio of 1:1, were dissolved in 70% ethanol. The solution was slowly dropped into the water which contains sodium caseinate as a stabilizer. The nanosuspension was concentrated by a rotary evaporator then centrifuged followed by freeze-drying. The encapsulation efficiency of DMY was reported at 90.2%. Zheng and Zhang [113] prepared the astilbin-encapsulated zein – caseinate nanoparticles. The bioavailability of astilbin was improved from 0.32 to 4.40% in rats through nanoparticle fabrication. Davidov-Pardo et al. [114] encapsulated the resveratrol into biopolymer via LASC. The hydrophobic polymers, gliadin and zein, were dissolved in a drug solution followed by its injection in the antisolvent medium. The effect of hydrophilic polymer (pectin and sodium casinate) in the antisolvent medium was studied on the encapsulation efficiency. The highest encapsulation efficiency was reported to be 86% for zein as hydrophobic and sodium casinate as hydrophilic polymer.

Effect of the process variables

The particle characteristics such as particle size, particle size distribution, and morphology can be controlled by tuning the process parameters. The drug concentration, mixing speed, solvent to antisolvent ratio, temperature, and solution injection rate are process parameters influencing the particle characteristics. The effects of these parameters on particle characteristics are discussed in the following section.

Effect of drug concentration

The drug concentration is an important factor to tune the particle size and particle size distribution. When a high concentration drug solution is injected into the antisolvent, it results in high supersaturation in the solvent-antisolvent mixture. The high supersaturation leads to a high nucleation rate resulting in a large number of nuclei and subsequently

Table 2 Stabilizers/additives used in LASC

API	Polymer/surfactant	Key finding	References
Fluconazole	PLF-127, KL, HPMC, XG, PVP, SLS	The average particle size of the nano-suspension was found 352 nm using PL F127 as a stabilizer	[25]
Tadalafil	Tween 80	The spherical particles with a mean size of 358.47 ± 11.95 nm were prepared at optimum conditions. The dissolution rate of the processed tadalafil nanocrystals in 120 min was significantly increased (3.61-fold) as compared to that of the raw material	[49]
Efavirenz	HPMC, PVP, SLS, HPC, poloxamer 188, poloxamer 407	The most stable suspension of efavirenz was produced using PVP as a stabilizer. The optimum concentration of PVP was 20% related to EFV mass	[63]
Sulfamethxole	HPMC,PAA, PVA,PVP, SDS	The lowest average particle size was obtained when the concentration of HPMC, PAA, PVA, and SDS were 0.3, 0.4, 0.2, and 0.1% (w/v) respectively. In the case of PVP, the particle size was larger and could not be measured	[64]
Griseofulvin	HPMC, Tween 80, PVP, BSA	The different additives led to different morphology such as umbrella-like, hexagonal, needle-like and six-branched hierarchal structures	[65]
Tamoxifen	α-D(+)-glucose penta acetate, Triton X-100, urea	Triton X-100 was found the most suitable additive to reduce the aspect ratio and particle size of tamoxifen	[68]
Telmisartan	SLS, poloxamer 188, Tween 80	The average particle size of the nanosuspension was 750 nm. Poloxamer 188 and Tween 80 were found suitable stabilizers	[73]
Loratadine	Poloxamer 188	The nanocrystal prepared by LASC was incorporated into mucoadhesive agent, sodium hyaluronate, for nasal delivery. An increase in 5.54-fold bioavailability was reported in nasal administration as compared to oral administration	[74]
Candesartan Cilexetil	PVP K-30, PVP K-90, SLS	The average particle size of 291.5 nm and 238.9 nm was reported when PVP K-30 and PVP K-90 were used as additives	[75]
trans-Cinnamic acid	HPMC	The average particle size of nanosuspension was 130 nm. The solubility, bioavailability, and dissolution rate of nano-sized particles increased by 3.33, 2.16, and 1.67 fold, respectively	[76]
Mefenamic acid	HPMC, DOSS, PVA	The nanosuspension was stabilized by adding stepwise additives. DOSS was followed by HPMC or PVA, during the crystallization process. A stable nanosuspension of mefenamic acid of the average particle size of 317 nm was obtained	[77]
Fenofibrate	PVP K30, Pluronic F127, PVA, HPMC, SDS, Kolliphor 188, PEG	PVA was the most effective stabilizer for producing stable submicron particles. The optimum concentration of PVA was found to be 0.2% (w/v)	[78]
Curcumin	SDS, HPMC, Tween 80	Nucleation kinetics was estimated in the presence of stabilizers. The use of the stabilizer was found to lower the nucleation rate and increase the induction time and metastable zone width	[79]
Resveratrol	PVP K17, poloxamer 188	The average particle size of nanosuspension was found 140 nm while the original particle size of resveratrol was 1–5 µm	[80]
Furosemide	Poloxamer	The increase in relative bioavailability was found to be 2.3-fold due to the enhanced solubility and dispersion rate of the drug from the nanosuspension formulation	[81]

Table 2 (continued)

API	Polymer/surfactant	Key finding	References
Tadalafil	HPMC, VA64, and PVP K-30	The solid dispersion obtained using the optimized process conditions exhibited 8.5-fold faster dissolution rates in the first minute of dissolution, 22-fold greater apparent solubility at 10 min, and a 3.67-fold increase in oral bioavailability than raw tadalafil	[82]
Glimepiride	HPMC, PVP K-30, SLS	LASC processed glimepiride dissolved 85% in the first 10 min as compared to 10.17% unprocessed drug	[83]
Lutein esters	Poloxamer 188	The solubility and dissolution rates of LE-NPs in artificial gastric juice were 12.75 and 9.65 times that of the raw LE, respectively	[84]
Budesonide	Tyloxapol	Methanol and acetone were used as a solvent. The rectangular shape was obtained from an acetone–water system while elliptic particles were obtained from a methanol–water system	[85]

SLS sodium lauryl sulphate, *PVP* polyvinylpyrrolidone, *HPMC* hydroxypropyl methylcellulose, *PAA* polyacrylic acid, *PVA* polyvinyl alcohol, *BSA* bovine serum albumin, *HPC* hydroxypropyl cellulose, *DOSS* sodium docusate, *PEG* polyethylene glycol, *SDS* sodium dodecyl sulfate

a decrease in the particle size. Zhang et al. [115] prepared the nanoparticle of soy isoflavone (SIF) and reported that the average particle size decreased from 208 to 110 nm as isoflavone concentration in dimethyl sulfoxide (DMSO) increased from 10 to 30 mg/ml. A similar trend of decreasing particle size with an increase in concentration was reported for betulin [106], silibinin [110], and benzoic acid [116]. However, an increase in drug concentration above a certain value may also lead to high agglomeration leading to large particle size. Lee et al. [117] prepared the bisacodyl nanoparticles using N-methyl-2-pyrrolidone (NMP) as a solvent. An increase in particle size from 131 to 831 nm was

Table 3 Liquid antisolvent crystallization using ionic liquid as solvent

Drug	Ionic liquid	Key finding	References
LASSBio-294	1-ethyl-3-methylimidazolium methyl phosphonate	The recrystallized LASSBio-294 had the same crystalline peaks as raw drugs. However, peak intensities were different due to changes in the orientation, morphologies, and particle size. The residual amount of solvent increased with the increase in drug solution concentration	[86]
Carbamazepine	Imidazolium [BMIM][C1]	The solubility of carbamazepine in imidazolium was 221 mg/ml compared to 18.9 mg/ml in ethanol and 92 mg/ml in methanol. The dihydrate (DH) carbamazepine from initial Form III (P-monoclinic) was formed after LASC which was most stable at room temperature and pressure	[87]
Paclitaxel	1-hexyl-3-methylimidazolium bromide (HMImBr)	The bioavailability of the LASC processed paclitaxel increased 10.88 fold than that of raw paclitaxel	[94]
Clopidogrel bisulfate	1,3-diallylimidazolium tetrafluoroborate (AAImBF4)	The control of polymorphic transformation from Form I to Form II was studied and confirmed	[95]
Adefovir dipivoxil	1-allyl-3-ethylimidazolium Tetrafluoroborate (AEImBF4)	A new form of adefovir dipivoxil crystals was formed at a temperature below 50 °C. This is attributed to the unique intermolecular interactions of adefovir dipivoxil molecules induced by the ionic liquid	[96]
Rifampicin	1-ethyl 3- methyl imidazolium methyl-phosphonate	The drug solubility was found at 90 mg/g in an ionic liquid. The amorphous particles with diameters 280–360 nm were obtained. The solubility of recrystallized rifampicin increased 30% (from 0.72 mg/g of raw rifampicin to 0.94 mg/g of nano-sized precipitated particles) due to particle size reduction and solid-state amorphization	[97]

Table 4 Herbal compounds processed by LASC

Compound	Solvent	Key findings	References
Resveratrol	Ethanol	The nanoparticles within the range of 100–250 nm were prepared. The dissolution rate of nanoparticles was approximately doubled compared with raw resveratrol	[101]
Licorice	Methanol	The saturation solubility of licorice nanoparticles was 24-fold of raw licorice. The dissolution rate of licorice nanoparticles was reported 9.36-fold higher in artificial intestinal juice and 11.66-fold higher in artificial gastric juice	[102]
Ginkgo biloba extract	Ethanol	The antioxidant activity and oral bioavailability of prepared nanoparticles were improved. The average particle size of nanoparticles was 76.90 nm at optimum conditions of LASC	[103]
Silibinin	Ethanol	LASC processed nanoparticles had a better pharmacokinetic profile in comparison to the unprocessed drug	[104]
Curcumin	Ethanol	The highest solubility of curcumin nanocrystals was observed when PEG 1500 was used as an additive. The optimized curcumin crystals yielded 7.8-fold higher bioavailability as compared to unprocessed curcumin	[105]
Betulin	Ethanol	The mean particle size of betulin was 110 nm at optimum values of process parameters. The bioavailability enhancement of 1.21-fold was reported as compared to raw betulin	[106]
Curcumin	Ethanol	A different polymorphic form (Form 3) was produced using ethanol as solvent and bovine serum albumin (BSA) as an additive	[107]
Apigenin	N, N-dimethyl-formamide (DMF)	The mean particle size of apigenin under optimum conditions was about 159.2 nm. The oral bioavailability of apigenin nanoparticles was reported to be 4.96-fold higher than that of raw apigenin	[108]
Glycyrrhetinic acid	Dimethyl Sulfoxide (DMSO)	The mean particle size of GA nanocrystals was reported to be 220 nm. The oral bioavailability of nanocrystals was 4.3-fold higher in rats when compared with coarse GA particles	[109]
Silibinin	Ethanol	The average particle size of silibinin nanoparticles was 132.9 nm. The dissolution rate of silibinin nanoparticles was about 48.2-fold and 153.8-fold that of free silibinin in artificial gastric juice and artificial intestinal juice respectively	[110]

reported by increasing the concentration (mole fraction) of bisacodyl in NMP from 0.02 to 0.06. The trend of increasing particle size with an increase in concentration was reported for simvastatin [26], nitrendipine [118], and bicalutamide [119]. Therefore, two opposing factors, supersaturation and agglomeration, determine the effect of concentration on particle size. Zu et al. [120] studied the effect of concentration (50, 100, 150, 200, and 250 mg/ml) for crystallization of l-nimodipine. The average particle size decreased when concentration increased from 50 to 150 mg/ml. After that, particle size increased with an increase in concentration from 200 to 250 mg/ml. Deshpande et al. [121] also observed a similar trend, a decrease followed by an increase in particle size with concentration, for glibenclamide (GLB) nanoprecipitation.

Effect of temperature

The solubility of pharmaceutical compounds generally increases with an increase in temperature as shown in Fig. 2 [122]. The high temperature means high solubility of a drug in a solvent-antisolvent mixture and subsequently low supersaturation. Temperature also influences the diffusion of drug molecules on existing nuclei. The high temperature enhances the diffusion process due to reduced viscosity and subsequently larger growth leading to an increase in the particle size [123]. The increase in temperature resulted in the larger particles for flufenamic acid [34], megestrol acetate [124], amphotericin B [125], danazol [126], irbesartan [127], phenylbutazone [128], and gliadin [129]. However, Zhao et al. [106] prepared the nanosuspension of betulin and reported that higher temperature leads to smaller particles. The mean particle sizes of betulin at temperatures 0, 10, 20, 30, and 40 °C were found to be 717.1, 638.3, 398.6, 380.2, and 292.5 nm, respectively. This is attributed to the effect of temperature on nucleation rate being significant compared to supersaturation as shown in Eq. (1).

$$B^o = A_{hom} \exp\left(-\frac{16\ \pi\ \gamma_{sl}^3 \upsilon^2}{3k^3T^2(ln(1+s))^2}\right) \quad (1)$$

where B^o is the nucleation rate, A_{hom} is the pre-exponential factor, γ_{sl} is the interfacial tension at the solid–liquid interface, ν is the molar volume, and T is the temperature.

Effect of the ratio of solvent to antisolvent (S/AS)

The ratio of solvent to antisolvent (S/AS) was found to affect the particle size, particle size distribution, and consequently

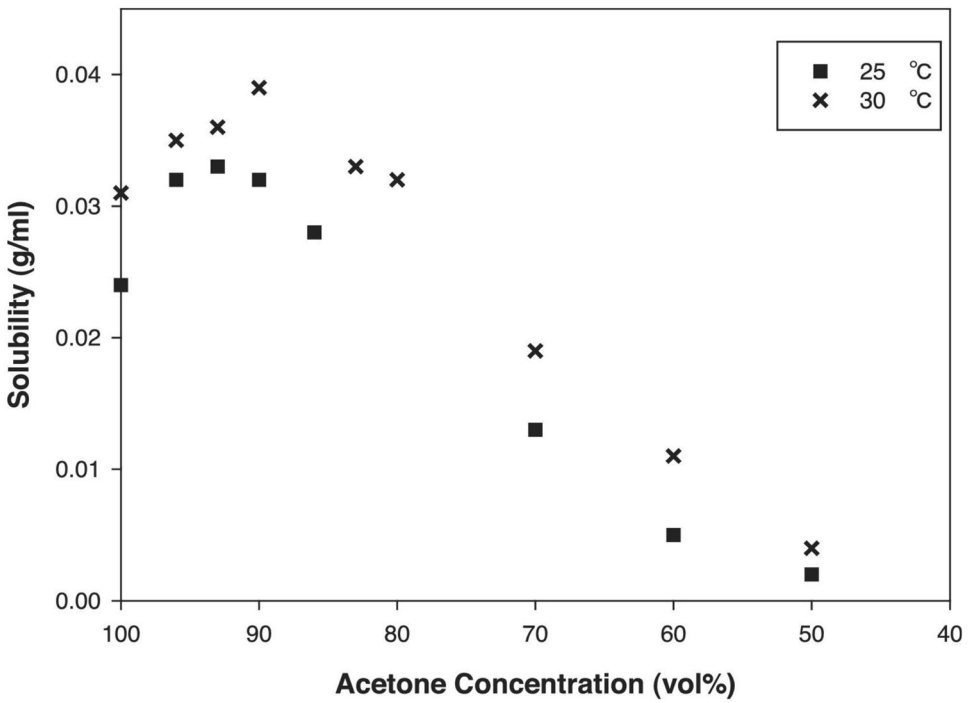

Fig. 2 Solubility of griseofulvin in acetone/water mixture vs acetone concentration in the mixture. Reprinted with permission from [122]. Copyright Elsevier, 2015

the stability of the nanosuspension. The S/AS ratio is generally maintained from 1: 5 to 1:20 in LASC. An increase in the antisolvent leads to a rapid reduction in the equilibrium solubility of the drug followed by high supersaturation. The high supersaturation results in a high nucleation rate and subsequently a decrease in the average size of nanoparticles. The high antisolvent amount also increases the diffusion distance for molecules to grow the nuclei [130]. A higher diffusion distance means a reduction in particle size and diffusion becomes the controlling step for particle growth. The reduction in particle size with an increase in the S/AS was reported for betulin [106], simvastatin [26], nimesulide [131], and glibenclamide [132]. However, the high antisolvent amount may also lead to poor mixing and therefore large particles. Deshpande et al. [121] studied glibenclamide (GLB) nanoprecipitation and found that particle size first decreases and then increases with an increase in S/AS ratio. A similar trend was also observed during the preparation of cinnarizine nanosuspension [133].

Effect of solution injection rate

The solution injection rate is one of the vital factors to tailor the average particle size and particle size distribution. At a higher solution injection rate, the mixing between solution and antisolvent is fast leading to high supersaturation. Therefore, higher solution injection rate will lead to the formation of a larger number of nuclei and subsequently smaller particles. A decrease in the particle size with an increase in the drug injection rate was reported for flufenamic acid [34], phenylbutazone [128]. A low micromixing efficiency leads to uneven supersaturation and subsequently larger particle size and broad particle size distribution [131]. In a continuous liquid antisolvent process, the solution and antisolvent are injected together into a mixing platform such as milichannels or microfluidic devices. Zhu et al. [134] studied the effect of overall volumetric flow rate (sum of solution and antisolvent flow rates) on the average particle size of cefuroxime axetil particles. They reported that a higher overall volumetric flow rate leads to a higher Reynolds number. At a high Reynolds number, turbulence becomes strong which leads to better micromixing between drug solution and antisolvent. Therefore, a decrease in particle size from 760 to 440 nm was reported with an increase in the total flow rate from 1.5 to 6 L/min.

Effect of solution/antisolvent injection

In most of the experiments, the drug solution is injected into antisolvent to carry out the crystallization process. When drug solution is injected into antisolvent, a high supersaturation is generated due to the high mole fraction of antisolvent in the binary mixture of solvent-antisolvent. The high supersaturation results in a high nucleation rate and subsequently smaller particles [135]. The effect of antisolvent addition to the drug solution on particle size has also been explored [136]. Park et al. [136] observed that the average particle size of sulfabenzamide was larger when water was injected into the drug solution. This is attributed to the low value of supersaturation leading to slow nucleation.

Continuous antisolvent crystallization

Pharmaceutical crystallization is conventionally carried out on a batch-wise basis [137]. The major drawbacks of the batch process are larger inventories, high footprint, higher probability of product contamination, higher requirements of human intervention, reduced material and energy usage, product variability from batch to batch, and higher product cost [138–140]. The continuous crystallizers overcome these drawbacks of the batch crystallization process. One major advantage of using continuous manufacturing is to reduce solvent usage in pharmaceutical crystallization which is the major source of environmental waste [140].

Mixed suspension mixed product removal (MSMPR) crystallizers operating in continuous mode can overcome some of the problems associated with batch production mode. However, the limitation of MSMPR crystallizers is the long residence time leading to broader particle size distribution [139]. The continuous flow crystallizers (PFCs) are an attractive approach enabling control over product characteristics in a highly reproducible manner [141]. Solymosi et al. [142] studied the liquid-antisolvent process in batch and continuous flow crystallizers. They reported that the LASC can be easily intensified and scaled up in continuous flow as compared to the batch process. This is attributed to uniform mixing in the continuous flow system.

Benitez-Chapa et al. [139] studied the continuous crystallization of flufenamic acid using a coiled flow inverter (CFI) crystallizer with a multistage addition antisolvent strategy. The different configuration of CFI was used as shown in Fig. 3. The number of bends was found to be the most important factor to produce the narrow particle size distribution. Hussain et al. [143] studied the crystallization of acetyl salicylic acid using ultrasound in a tubular flow crystallizer. They reported the redissolution of crystals due to temperature rise in the flow crystallizer. This is overcome by using low-power ultrasound or a cooling bath in the crystallizer. The advantage of using ultrasound in a flow reactor is the short induction time and fast nucleation [144]. As APIs have typically high molecular complexity and slow nucleation kinetics [145], the use of ultrasound in tubular crystallizers is an attractive approach for pharmaceutical crystallization. Ferguson et al. [146] reported that the PFC is capable of producing particles with narrow size distribution in a highly reproductive manner. However, the application of the PFC requires fast crystallization kinetics to ensure the process reaches completion in a residence time. Therefore, the use of ultrasound in LASC is required to achieve fast nucleation kinetics and subsequently fine particles. Azad et al. [147] prepared the concentrated stable fenofibrate nanosuspension by combining T-mixer with a sonication probe.

The microfluidic-based anti-solvent crystallization has been explored for continuous and scalable production of nanoparticles. The advantage of a microfluidic environment includes laminar flow, intensified micro-mixing, and good temperature control. The intensified micro-mixing leads to a uniform spatial concentration distribution and a high value of supersaturation. Zhao et al. [126] reported that characteristic micromixing time (τ_m), a time for species reaching a maximum mixed state at the molecular level, is of the order of 5–50 ms in a stirred tank. This is much higher when compared with the characteristic micromixing time for the microchannel which is in the range of 0.25–0.35 ms. Due to this reduction in characteristic micromixing time, Zhao et al. [126] successfully prepared the danazol nanoparticles in microfluidic-based LASC without the use of any additive. The variety in the design of the microfluidic device has been investigated to control the crystallization process and preparation of APIs nanoparticles with narrow particle size distribution [148, 149]. Shrimal et al. [150] prepared the nanosize particle of telmisartan in a tubular microchannel fabricated using a 0.8-mm ID silicon tube. The shape of the microchannel was serpentine to enhance the mixing. The nanoparticles with an average size of 369 nm were prepared at optimum conditions using Poloxamer 407 as the stabilizer.

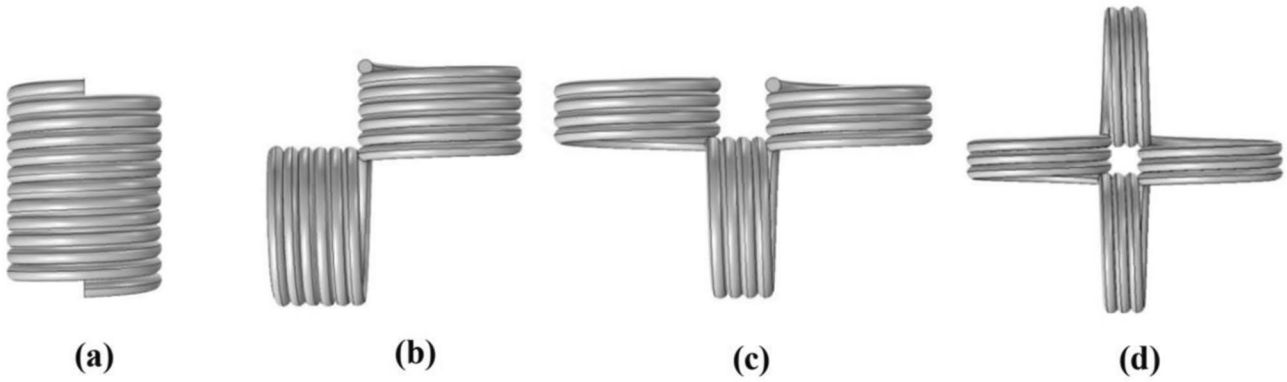

Fig. 3 Geometries of CFI used **a** helical, **b** one 90-degree bend, **c** two 90-degree bends, **d** three 90-degree bends. Reprinted with permission from [139]. Copyright American Chemical Society, 2019

Chen et al. [151] used a T-shape micro-channel to prepare the nanoparticles of itraconazole. The poor mixing was observed at 5 °C while complete mixing was observed in the temperature range of 25–80 °C. The control over mixing between solvent and antisolvent phase enables the tuning of the particle size. Le et al. [152] explored the acoustically enhanced microfluidic mixer to prepare the nanoparticle of budesonide. They successfully prepared the nanoparticles without using any additives. Rahimi et al. [153] prepared the curcumin nanoparticles using microfabricated channels with three different junction angles (θ = 45, 90, 135 degrees) as shown in Fig. 4. The average curcumin nanoparticle size of 175 nm was obtained at θ = 135 degrees. This was attributed to the efficient mixing at this injection angle. This was also validated by the computational fluid dynamics simulation.

Zhu et al. [134] prepared the nanosized cefuroxime axetil (CFA) using a high-throughput microporous tube-in-tube microchannel reactor (MTMCR). High throughput in the range of 1.5–6 L/min was achieved in MTMCR which shows its potential for industrial application. A schematic diagram of MTMCR is shown in Fig. 5. The micropore zone is made up of metal mesh with a size range from 5 to 80 µm. The annular channel width is in the range of 500–1500 µm. The author reported that average particle size decreased from 1000 to 420 nm as micropore size decreased from 80 to 5 µm. The average particle size was reduced from 920 to 360 nm by changing the annular channel width from 1500 to 500 µm.

LASC-based combinative techniques

The combination of LASC with other techniques has also been explored for particle size reduction of pharmaceutical compounds. Hu et al. [154] investigated the technical feasibility of nanoparticle preparation by coupling the LASC with immediate drying as shown in Fig. 6. Fenofibrate was used as a model drug, lactose/mannitol as matrix former, and hydroxylpropylmethyl cellulose (HPMC)/sodium dodecyl sulfate (SDS) as stabilizers. The authors claimed to produce 10 g of drug nanoformulation in 1 h. The product exhibited a significantly higher dissolution rate with 84.2% drug dissolved in 5 min as compared to the conventional spray-dried formulation (31.7%) and the physical mixture (9.7%) using micronized fenofibrate. This combination approach has the potential for continuous large-scale production of nanoformulation. Recently, Hu et al. [155] prepared the budesonide nanoparticle embedded in mannitol by the same approach to enhance the dissolution rate and bioavailability of the drug. Dong et al. [156] studied the spray drying of nanosuspension of fenofibrate produced via LASC. They observed that a clay, montmorillonite (MMT), is a better matrix former as compared to sugars (e.g., lactose, sucrose). This is due to the incapability of sugars to prevent the nanoparticle agglomeration in suspension.

Gu et al. [157] explored the combination of antisolvent precipitation and high-pressure homogenization followed by lyophylization to prepare vitexin nanopowder. The mean particle size of vitexin nanoparticles prepared by LASC was 368.4 ± 31.23 nm. This nanosuspension is further processed by high-pressure homogenization which reduced the average particle size to 80 nm at optimum conditions. Zhang et al. [158] prepared the baicalein nanocrystals by anti-solvent recrystallization followed by high-pressure homogenization. The advantage of using LASC as a pretreatment step is to prevent the blocking of the homogenizer gap. The baicalein nanocrystals of 335 nm were produced by this combinative approach.

Xu et al. [159] prepared the ultrafine particles of beclomethasone dipropionate (BDP) by combining microfluidic antisolvent crystallization, high-pressure homogenization (HPH), and spray drying. The needle-shaped particles

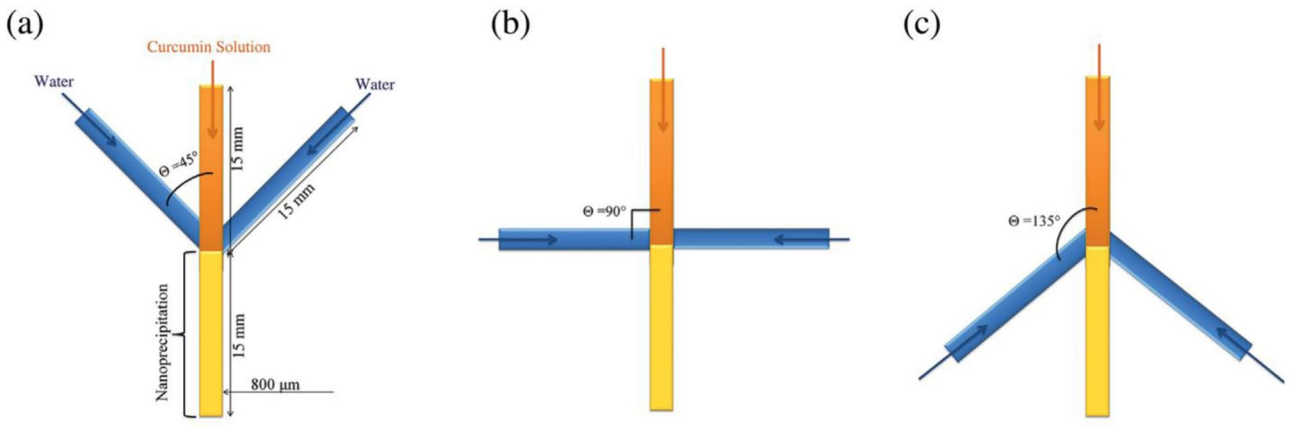

Fig. 4 Schematic of microfluidic devices with three different junction angles **a** θ = 45 degree, **b** θ = 90 degree, **c** θ = 135 degree. Reprinted with permission from [153]. Copyright John Wiley and Sons, 2017

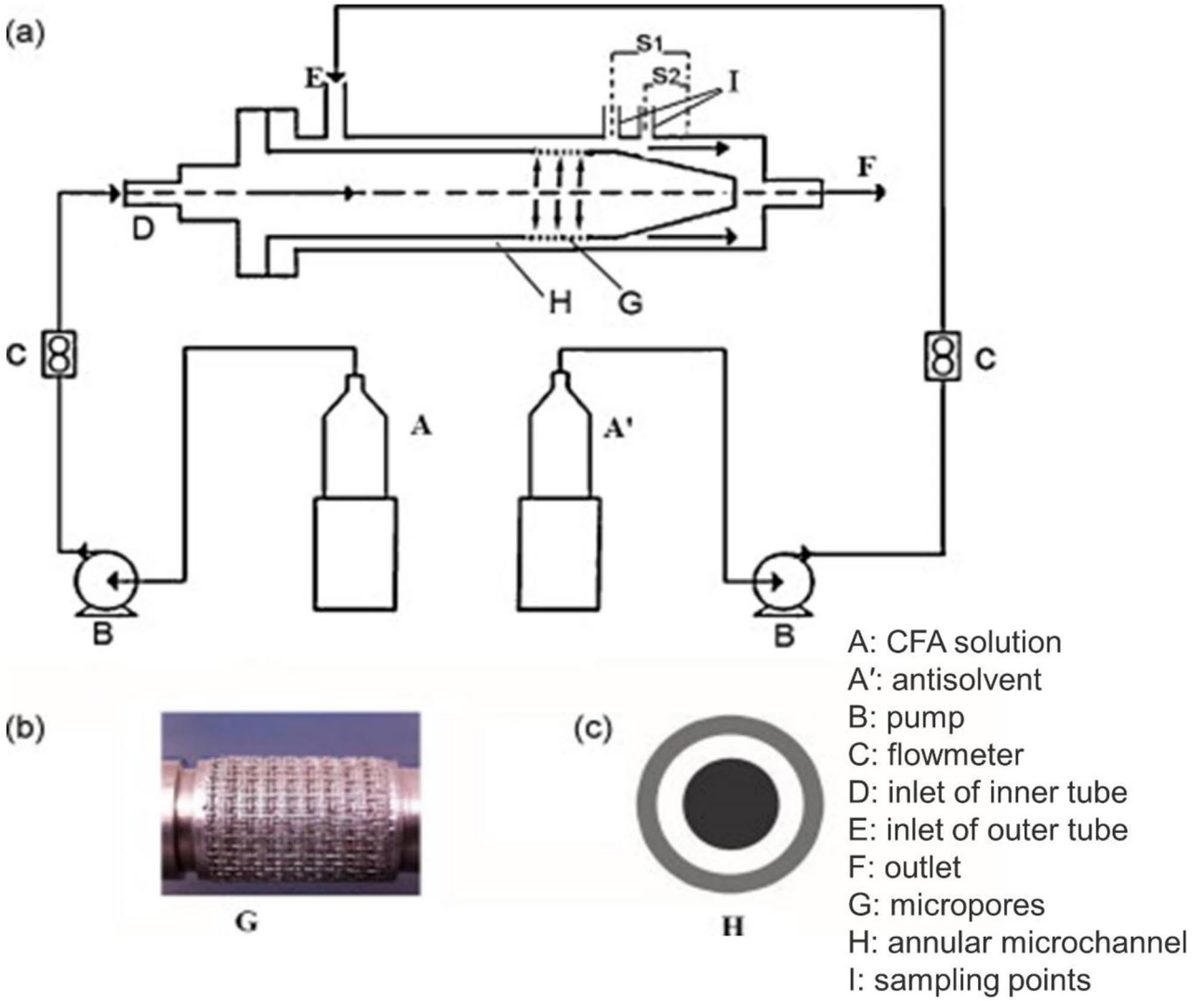

Fig. 5 **a** Schematic diagram of MTMCR experimental set-up, **b** photograph of micropore section, **c** profile of the annular microchannel. Reproduced with permission from [134]. Copyright Elsevier 2010.

were prepared by antisolvent crystallization which was broken down into smaller particles by high-pressure homogenization. The suspension from high-pressure homogenization was dried into uniform low-density spherical BDP aggregates by spray drying. The BDP particles of average size 2–3 µm were obtained after spray drying. The product has an excellent aerosol performance, 2.8- and 1.4-fold higher than the raw BDP, and vacuum-dried BDP particles, respectively.

Kumar et al. [160] prepared the nano-amorphous powder of itraconazole using LASC followed by spray drying. Spray drying of the nano-precipitated formulation was performed with several auxiliary excipients to obtain a nano-sized amorphous powder. They reported superior performance in in vitro dissolution testing and in vivo studies of nano-amorphous formulations compared to melt-quench amorphous and crystalline itraconazole formulations. Ma et al. [161] prepared nano-sized valsartan using LASC followed by spray drying. The spray-dried nanoparticles were in an amorphous state. The oral bioavailability in rats was reported to be 2.5-fold higher compared to commercial products. Zhong et al. [162] combined the reactive precipitation with a liquid antisolvent crystallization process to prepare the nanoparticle of cephradine. The nanoparticles of an average size of 300 nm were successfully prepared by this combination technique.

Comparison of LASC with other techniques

Recently, Pandey et al. [163] studied the LASC and self-nanoemulsifying drug delivery system (SNEDDS) to enhance the dissolution rate, solubility, and

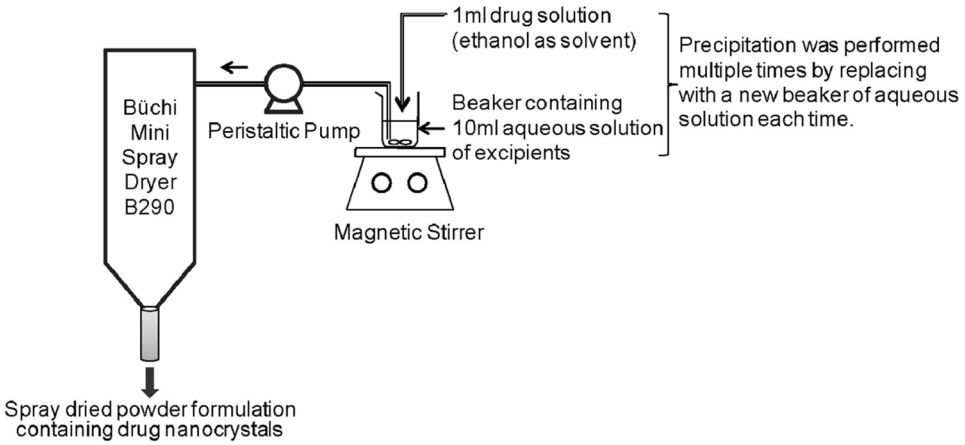

Fig. 6 Schematic of LASC coupled with spray drying. Reprinted with permission from [154]. Copyright Elsevier 2011

bioavailability. The increase in the bioavailability of glimepiride was reported at 6.69- and 4.22-folds for the LASC- and SNEDDS-processed drugs, respectively. This shows that the LASC process is more suitable for glimepiride. Mahesh et al. [164] studied the preparation of glipizide nanoparticles by media milling and liquid anti-solvent crystallization method. The glipizide nanosuspension prepared by LASC exhibited a higher dissolution rate (98.97%) as compared to the nanosuspension (96.44%) prepared by media milling. However, the effect of aging was observed for nanosuspension prepared by LASC. Zhang et al. [165] prepared the fenofibrate nanocrystals by liquid antisolvent process and thermal precipitation method. The oral bioavailability of fenofibrate nanocrystals produced by LASC and the thermal precipitation method was found at 5.5- and 5-folds, respectively. Bolourchian et al. [166] compared the cooling and antisolvent crystallization to enhance the dissolution rate of meloxicam. A significant improvement in dissolution rate was observed when meloxicam particles were precipitated by the antisolvent technique (2.5-fold higher than the raw meloxicam) as compared to cooling crystallization (1.6-fold higher than the raw meloxicam). This is attributed to fast nucleation, lower particle size, higher wettability, and less aggregation of meloxicam particles.

Yeo et al. studied the crystallization of sulfamethizole using liquid antisolvent crystallization and the supercritical CO2-based antisolvent crystallization process [167]. Liquid antisolvent crystallization was carried out in the absence and presence of ultrasound. The effect of slow and rapid injection rate of carbon dioxide was also investigated. The application of ultrasound in LASC process resulted in particle size and particle size distribution of the same order as obtained by the supercritical CO2-based antisolvent crystallization process as shown in Fig. 7. This signifies that LAS can become an attractive alternative to high-cost supercritical antisolvent crystallization.

Future perspectives

Although most of the studies focused on the preparation of nanoparticles of different drugs, some researchers have also studied the application of LASC in diverse fields of pharmaceutical research. The applications of LASC in the following research area are less explored and require the attention of researchers.

LASC can be used to prepare the inclusion complex of APIs. Wu et al. [168] prepared the inclusion complex of apigenin with 2-hydroxypropyl-β-cyclodextrin prepared using LASC and solvent removal method. The product apigenin had a higher solubility of 6.19 mg/ml as compared to the raw apigenin (1.93 mg/ml). This approach could be useful for those pharmaceutical compounds which have low solubility in organic solvents.

LASC is also reported to yield the different polymorphs by changing the solvent. Pandey et al. [169] produced monoclinic (Form 1) and orthorhombic Form 3 of curcumin using acetone and dimethyl sulfoxide as solvents respectively. Form 3 exhibited a higher propensity for transdermal drug delivery as compared to monoclinic curcumin (Form 1).

Antisolvent crystallization has been studied to improve the flow properties and compression behavior of API. Kedia and Wairkar [170] studied the antisolvent crystallization of cycloserine, a high-dose antitubercular drug, using water as solvent and 1-butanol as anti-solvent. They reported that LASC can be explored to improve the flowability and compressibility of large-dose oral drugs.

Azad et al. [171] prepared the biocompatible film from the precipitated suspension of fenofibrate via the liquid antisolvent process. The authors observed the high drug loading (20%) as compared to the film prepared by incorporating the FNB nanoparticle via melt emulsification. Chandra et al. [172] prepared fast-dissolving film strips containing lacidipine nanoparticles produced via LASC

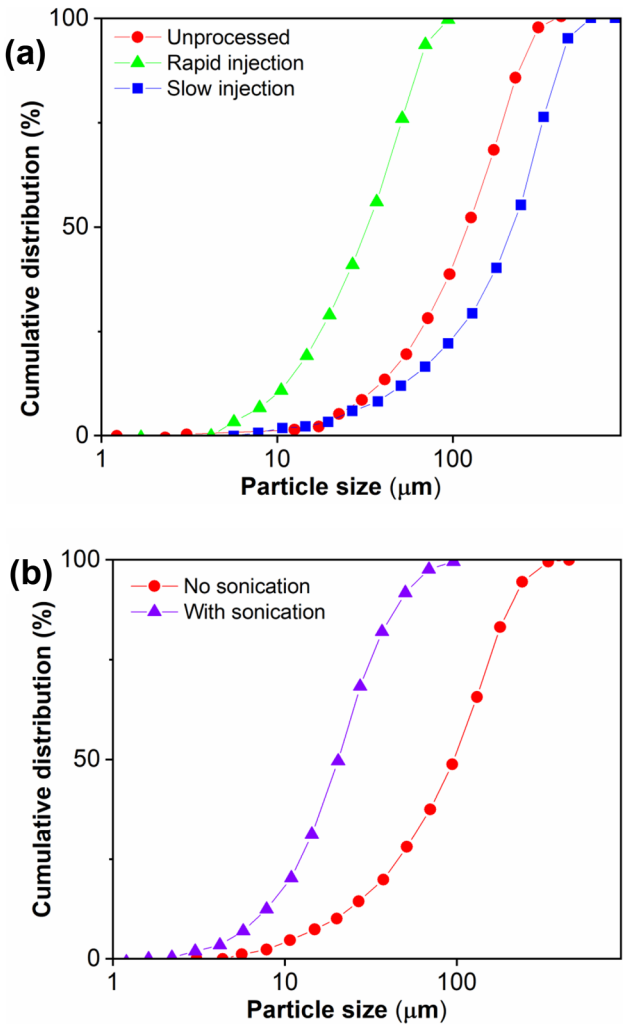

Fig. 7 Cumulative size distribution of sulfamethizole crystals: (**a**) supercritical CO2-based antisolvent crystallization experiments at 50 °C and (**b**) LASC experiments with and without sonication at 30 °C. Reprinted with permission from [167]. Copyright Elsevier 2004

for transbuccal administration and therefore the potential to overcome the low oral bioavailability problem associated with the administration of lacidipine. The prepared film was reported to have a sufficiently high dissolution rate as compared to raw lacidipine. However, Beck et al. [173] prepared the strip film of griseofulvin (GF) particles precipitated via LASC and reported low drug concentration in the film. The preparation of biocompatible film using particles produced via LAS needs to be explored.

The loading of drug nanoparticles into polymers by the liquid antisolvent process is one of the areas to be explored. Wu et al. [174] loaded silibinin in porus starch to improve the solubility and bioavailability. The higher solubility of drug-loaded nanoparticles as compared with free drugs or nanoparticles was observed.

LAS crystallization has been explored to produce the nanoparticles of the compounds used in the food system [175]. For water-soluble proteins, antisolvent crystallization can be carried out using other nonsolvents. Albumin and gelatin, the highly water-soluble proteins, were nano-precipitated using alcohol and acetone as antisolvents [176, 177]. Nanoprecipitation of proteins using LASC can be further studied by future researchers.

Conclusion

Liquid antisolvent crystallization is one of the promising approaches to prepare the nanoparticles of pharmaceutical/herbal compounds. The use of ultrasound and additives in LAS crystallization can result in stable nanosuspension. Ultrasound reduces the induction time which leads to a fast nucleation rate and subsequently fine particles. LASC usually results in needle-shaped particles due to rapid growth in one direction. The surfactant type and its concentration play a vital role in tuning the particle characteristics. The selection of stabilizer and its optimum quantity plays a major role in the formulation of the nanosuspension of APIs. The LASC is carried out either in a stirred vessel or a continuous flow channel. Due to the inherent disadvantages of batch crystallization, plug flow crystallizers are an attractive alternative for antisolvent crystallization. The microfluidic-based antisolvent crystallization approach was successful to prepare the nanoparticles with very high reproducibility. The combination of LASC with other techniques such as high-pressure homogenization or spray drying is also suitable to tune the average particle size. LASC with ultrasound is capable of producing particles of the same size and size distribution as compared to the supercritical carbon dioxide-based antisolvent crystallization process. An economical comparison of LASC and supercritical carbon dioxide-based antisolvent crystallization can be assessed. The complete removal of solvent from the product is a major challenge. The presence of residual solvent may lead to the physical or chemical instability of the formulation. Besides the nanosize particles generation, some areas mentioned in the future perspective need to be explored by prospective researchers.

Acknowledgements The authors acknowledge their respective organizations for permitting to do this work.

Author contribution Dr. Rahul Kumar took a lead in writing this manuscript. Dr. Amit K. Thakur wrote the nanonization of herbal drugs. Dr. Nilanjana Banerjee revised the section "Comparison of LASC and other techniques." Dr. Ashutosh Kumar wrote the combinative approach. Dr. Gajendra Kumar Gaurav edited the original draft of manuscript. Dr. Nilanjana Banerjee and Dr. Raj Kumar Arya did editing of the revised version of the manuscript.

Data availability Not applicable.

Declarations

Ethics approval and consent to participate Not applicable.

Consent for publication Not applicable.

Competing interests The authors declare no competing interests.

References

1. Amidon GL, Lennernäs H, Shah VP, Crison JR. A theoretical basis for a biopharmaceutic drug classification: the correlation of in vitro drug product dissolution and in vivo bioavailability. Pharm Res. 1995;413–20.
2. Liu Q, Mai Y, Gu X, Zhao Y, Di X, Ma X, et al. A wet-milling method for the preparation of cilnidipine nanosuspension with enhanced dissolution and oral bioavailability. J Drug Deliv Sci Technol. 2020;55:101371.
3. Velický M, Tam KY, Dryfe RAW. In situ artificial membrane permeation assay under hydrodynamic control: correlation between drug in vitro permeability and fraction absorbed in humans. Eur J Pharm Sci. 2011;44:299–309.
4. Shekhawat P, Bagul M, Edwankar D, Pokharkar V. Enhanced dissolution/caco-2 permeability, pharmacokinetic and pharmacodynamic performance of re-dispersible eprosartan mesylate nanopowder. Eur J Pharm Sci. 2019;132:72–85.
5. Song S, Wang C, Wang S, Siegel RA, Sun CC. Efficient development of sorafenib tablets with improved oral bioavailability enabled by coprecipitated amorphous solid dispersion. Int J Pharm. 2021;610:121216.
6. Lentz KA, Plum J, Steffansen B, Arvidsson PO, Omkvist DH, Pedersen AJ, et al. Predicting in vivo performance of fenofibrate amorphous solid dispersions using in vitro non-sink dissolution and dissolution permeation setup. Int J Pharm. 2021;610:121174.
7. Müller M, Wiedey R, Hoheisel W, Serno P, Breitkreutz J. Impact of co-administered stabilizers on the biopharmaceutical performance of regorafenib amorphous solid dispersions. Eur J Pharm Biopharm. 2021;169:189–99.
8. Ijaz QA, Latif S, Shoaib Q, Rashid M, Arshad MS, Hussain A, et al. Preparation and characterization of ph-independent sustained-release tablets containing hot melt extruded solid dispersions of clarithromycin: tablets containing solid dispersions of clarithromycin. AAPS PharmSciTech. 2021;22:1–12.
9. Koli AR, Ranch KM, Patel HP, Parikh RK, Shah DO, Maulvi FA. Oral bioavailability improvement of felodipine using tailored microemulsion: surface science, ex vivo and in vivo studies. Int J Pharm. 2021;596:120202.
10. Mena-Hernández J, Jung-Cook H, Llaguno-Munive M, García-López P, Ganem-Rondero A, López-Ramírez S, et al. Preparation and evaluation of mebendazole microemulsion for intranasal delivery: an alternative approach for glioblastoma treatment. AAPS PharmSciTech. 2020;21:1–12.
11. Shah N, Seth A, Balaraman R, Sailor G, Javia A, Gohil D. Oral bioavailability enhancement of raloxifene by developing microemulsion using D-optimal mixture design: optimization and in-vivo pharmacokinetic study. Drug Dev Ind Pharm. 2018;44:687–96.
12. Seok SH, Lee SA, Park ES. Formulation of a microemulsion-based hydrogel containing celecoxib. J Drug Deliv Sci Technol. 2018;43:409–14.
13. Shinde UA, Modani SH, Singh KH. Design and development of repaglinide microemulsion gel for transdermal delivery. AAPS PharmSciTech. 2018;19:315–25.
14. Pinto LMA, Adeoye O, Thomasi SS, Francisco AP, Carvalheiro MC, Cabral-Marques H. Preparation and characterization of a synthetic curcumin analog inclusion complex and preliminary evaluation of in vitro antileishmanial activity. Int J Pharm. 2020;589:119764.
15. Špehar TK, Pocrnić M, Klarić D, Bertoša B, Čikoš A, Jug M, et al. Investigation of praziquantel/cyclodextrin inclusion complexation by NMR and LC-HRMS/MS: mechanism, solubility, chemical stability, and degradation products. Mol Pharm. 2021;18:4210–23.
16. Sherje AP, Kulkarni V, Murahari M, Nayak UY, Bhat P, Suvarna V, et al. Inclusion complexation of etodolac with hydroxypropyl-beta-cyclodextrin and auxiliary agents: Formulation characterization and molecular modeling studies. Mol Pharm. 2017;14:1231–42.
17. Li Y, He ZD, Zheng QE, Hu C, Lai WF. Hydroxypropyl-β-cyclodextrin for delivery of baicalin via inclusion complexation by supercritical fluid encapsulation. Molecules. 2018;23.
18. Araújo GP, Martins FT, Taveira SF, Cunha-Filho M, Marreto RN. Effects of formulation and manufacturing process on drug release from solid self-emulsifying drug delivery systems prepared by high shear mixing. AAPS PharmSciTech. 2021;22.
19. Khanfar M, Al-Nimry S, Attar S. Solid self nano-emulsifying system for the enhancement of dissolution and bioavailability of Prasugrel HCl: in vitro and in vivo studies. Pharm Dev Technol. 2021;26:1021–33.
20. Mahajan S, Singh D, Sharma R, Singh G, Bedi N. pH-independent dissolution and enhanced oral bioavailability of aripiprazole-loaded solid self-microemulsifying drug delivery system. AAPS PharmSciTech. 2021;22.
21. Assi RA, Abdulbaqi IM, Ming TS, Yee CS, Wahab HA, Asif SM, et al. Liquid and solid self-emulsifying drug delivery systems (Sedds) as carriers for the oral delivery of azithromycin: Optimization, in vitro characterization and stability assessment. Pharmaceutics. 2020;12:1–29.
22. Fu X, Xu S, Li Z, Chen K, Fan H, Wang Y, et al. Enhanced intramuscular bioavailability of cannabidiol using nanocrystals: formulation, in vitro appraisal, and pharmacokinetics. AAPS PharmSciTech. 2022;23:1–12.
23. Sodeifian G, Sajadian SA, Derakhsheshpour R. CO2 utilization as a supercritical solvent and supercritical antisolvent in production of sertraline hydrochloride nanoparticles. J CO2 Util. 2022;55:101799.
24. Zhu Y, Fu Y, Zhang A, Wang X, Zhao Z, Zhang Y, et al. Rod-shaped nintedanib nanocrystals improved oral bioavailability through multiple intestinal absorption pathways. Eur J Pharm Sci. 2022;168.
25. El Sayeh F, Abou El Ela A, Abbas Ibrahim M, Alqahtani Y, Almomen A, Sfouq Aleanizy F. Fluconazole nanoparticles prepared by antisolvent precipitation technique: physicochemical, in vitro, ex vivo and in vivo ocular evaluation. Saudi Pharm J. 2021;29:576–85.
26. Jiang T, Han N, Zhao B, Xie Y, Wang S. Enhanced dissolution rate and oral bioavailability of simvastatin nanocrystal prepared by sonoprecipitation. Drug Dev Ind Pharm. 2012;38:1230–9.
27. Kumar R, Thakur AK, Chaudhari P, Banerjee N. Particle size reduction techniques of pharmaceutical compounds for the enhancement of their dissolution rate and bioavailability. J Pharm Innov. 2021;1–20.
28. Rabinow BE. Nanosuspensions in drug delivery. Natur Rev Drug Discov. 2004;9:785–96.

29. Kesisoglou F, Mitra A. Crystalline nanosuspensions as potential toxicology and clinical oral formulations for BCS II/IV Compounds. AAPS J. 2012;14:677–87.
30. Müller RH, Gohla S, Keck CM. State of the art of nanocrystals - special features, production, nanotoxicology aspects and intracellular delivery. Eur J Pharm Biopharm. 2011;1–9.
31. Fontana F, Figueiredo P, Zhang P, Hirvonen JT, Liu D, Santos HA. Production of pure drug nanocrystals and nano co-crystals by confinement methods. Adv Drug Deliv Rev. 2018;131:3–21.
32. Kumar R, Thakur AK, Banerjee N, Chaudhari P. Investigation on crystallization phenomena with supercritical carbon dioxide (CO2) as the antisolvent. Int J Chem React Eng. 2021;19:861–71.
33. Kumar R, Thakur AK, Banerjee N, Chaudhari P. A critical review on the particle generation and other applications of rapid expansion of supercritical solution. Int J Pharm. 2021;121089.
34. Kumar R, Kumar S, Chaudhari P, Thakur AK. Liquid antisolvent recrystallization and solid dispersion of flufenamic acid with polyvinylpyrrolidone K-30. Int J Chem React Eng. 2021;19:663–71.
35. Sinha B, Müller RH, Möschwitzer JP. Bottom-up approaches for preparing drug nanocrystals: formulations and factors affecting particle size. Int J Pharm. 2013;126–41.
36. Yu G, Zhu H, Huang Y, Zhang X, Sun L, Wang Y, et al. Preparation of Daidzein microparticles through liquid antisolvent precipitation under ultrasonication. Ultrason Sonochem. 2021;79:105772.
37. McGinty J, Chong MWS, Manson A, Brown CJ, Nordon A, Sefcik J. Effect of process conditions on particle size and shape in continuous antisolvent crystallisation of lovastatin. Curr Comput-Aided Drug Des. 2020;10:1–17.
38. Ha ES, Park H, Lee SK, Jeong JS, Kim JS, Kim MS. Solubility, solvent effect, and modelling of oxcarbazepine in mono-solvents and N-methyl-2-pyrrolidone + water solvent mixtures at different temperatures and its application for the preparation of nanosuspensions. J Mol Liq. 2021;339:116792.
39. Thakur AK, Kumar R, Vipin Kumar VK, Kumar A, Kumar Gaurav G, Naresh GK. A critical review on thermodynamic and hydrodynamic modeling and simulation of liquid antisolvent crystallization of pharmaceutical compounds. J Mol Liq. 2022;362:119663.
40. Yuan N, Chen Z, Suo Z, Cheng Q, Sun Q, Li Y, et al. Solubility measurement, thermodynamic modeling, and molecular dynamic simulation of regorafenib in pure and binary solvents. J Chem Thermodyn. 2022;167.
41. Chen S, Liu Q, Dou H, Zhang L, Pei L, Huang R, et al. Solubility and dissolution thermodynamic properties of Mequindox in binary solvent mixtures. J Mol Liq. 2020;303:112619.
42. Oberoi D, Shankar U, Dagar P, Sahu S, Bandyopadhyay A. Electrochromic and bipolar memory switching properties of novel Eu(III)-polymer of multidentate Schiff's base ligand. J Mater Sci Mater Electron. 2020;31:20345–59.
43. Shankar U, Sethi SK, Singh BP, Kumar A, Manik G, Bandyopadhyay A. Optically transparent and lightweight nanocomposite substrate of poly(methyl methacrylate-co-acrylonitrile)/MWCNT for optoelectronic applications: an experimental and theoretical insight. J Mater Sci. 2021;56:17040–61.
44. Shankar U, Gupta CR, Oberoi D, Singh BP, Kumar A, Bandyopadhyay A. A facile way to synthesize an intrinsically ultraviolet-C resistant tough semiconducting polymeric glass for organic optoelectronic device application. Carbon N Y Pergamon. 2020;168:485–98.
45. Li T, Zhu L, Li J, Cao Z, Sha J, Li Y, et al. Solubility, thermodynamic properties and molecular simulation of tinidazole in fourteen mono-solvents at different temperatures. J Chem Thermodyn. 2022;170.
46. Kumar R, Rawat DS, Thakur AK, Chaudhari P, Banerjee N. Experimental measurement and thermodynamic modeling of solubility of flufenamic acid in different pure solvents. Mater Today Proc. 2022;57:1489–93.
47. Pabba S, Kumari A, Ravuri MG, Thella PK, Satyavathi B, Shah K, et al. Experimental determination and modelling of the co-solvent and antisolvent behaviour of binary systems on the dissolution of pharma drug; L-aspartic acid and thermodynamic correlations. J Mol Liq. 2020;314:113657.
48. Rathi N, Paradkar A, Gaikar VG. Polymorphs of curcumin and its cocrystals with cinnamic acid. J Pharm Sci. 2019;108:2505–16.
49. Rad RT, Mortazavi SA, Vatanara A, Dadashzadeh S. Enhanced dissolution rate of tadalafil nanoparticles prepared by sonoprecipitation technique: optimization and physicochemical investigation. Iran J Pharm Res. 2017;16:1335–48.
50. de Azevedo JR, Fabienne E, Jean-Jacques L, Inês RM. Antisolvent crystallization of a cardiotonic drug in ionic liquids: effect of mixing on the crystal properties. J Cryst Growth. 2017;472:29–34.
51. Valeh-e-Sheyda P, Rahimi M, Adibi H, Razmjou Z, Ghasempour H. An insight on reducing the particle size of poorly-water soluble curcumin via LASP in microchannels. Chem Eng Process Process Intensif. 2015;91:78–88.
52. Ramakers LAI, McGinty J, Beckmann W, Levilain G, Lee M, Wheatcroft H, et al. Investigation of metastable zones and induction times in glycine crystallization across three different antisolvents. Cryst Growth Des American Chemical Society. 2020;20:4935–44.
53. Wang X, Gillian JM, Kirwan DJ. Quasi-emulsion precipitation of pharmaceuticals. 1. Conditions for formation and crystal nucleation and growth behavior. Cryst Growth Des. 2006;6:2214–27.
54. Bhavna, Ahmad FJ, Mittal G, Jain GK, Malhotra G, Khar RK, et al. Nano-salbutamol dry powder inhalation: a new approach for treating broncho-constrictive conditions. Eur J Pharm Biopharm. 2009;71:282–91.
55. Hussain MN, Baeten S, Jordens J, Braeken L, Van Gerven T. Process intensified anti-solvent crystallization of o-aminobenzoic acid via sonication and flow. Chem Eng Process - Process Intensif. 2020;149:107823.
56. Gandhi NV, Deokate UA, Angadi SS. Development of nanonized nitrendipine and its transformation into nanoparticulate oral fast dissolving drug delivery system. AAPS PharmSciTech. 2021;22:1–15.
57. Lee J, Ashokkumar M, Kentish SE. Influence of mixing and ultrasound frequency on antisolvent crystallisation of sodium chloride. Ultrason Sonochem. 2014;21:60–8.
58. Cerdeira AM, Mazzotti M, Gander B. Miconazole nanosuspensions: influence of formulation variables on particle size reduction and physical stability. Int J Pharm. 2010;396:210–8.
59. Li M, Azad M, Davé R, Bilgili E. Nanomilling of drugs for bioavailability enhancement: a holistic formulation-process perspective. Pharmaceutics. 2016;8.
60. Trzenschiok H, Distaso M, Peukert W. A new approach for the stabilization of amorphous drug nanoparticles during continuous antisolvent precipitation. Chem Eng J. 2019;361:428–38.
61. Merisko-Liversidge E, Liversidge GG, Cooper ER. Nanosizing: a formulation approach for poorly-water-soluble compounds. Eur J Pharm Sci. 2003;18:113–20.
62. Lacerda S de P, Espitalier F, Hoffart V, Ré MI. Liquid anti-solvent recrystallization to enhance dissolution of CRS 74, a new antiretroviral drug. Drug Dev Ind Pharm. Informa Healthcare; 2015;41:1910–20.
63. Sartori GJ, Prado LD, Rocha HVA. Efavirenz dissolution enhancement IV—antisolvent nanocrystallization by sonication, physical stability, and dissolution. AAPS PharmSciTech. 2017;18:3011–20.
64. Kumar R, Siril PF. Drop-by-drop solvent hot antisolvent interaction method for engineering nanocrystallization of

sulfamethoxazole to enhanced water solubility and bioavailability. J Drug Deliv Sci Technol. 2020;55:101359.
65. Prasad R, Dalvi SV. Understanding morphological evolution of griseofulvin particles into hierarchical microstructures during liquid antisolvent precipitation. Cryst Growth Des. 2019;19:5836–49.
66. Rangaraj N, Pailla SR, Chowta P, Sampathi S. Fabrication of ibrutinib nanosuspension by quality by design approach: intended for enhanced oral bioavailability and diminished fast fed variability. AAPS PharmSciTech. 2019;20:1–18.
67. Pandey KU, Poornachary SK, Dalvi SV. Insights to the action of additives for stabilization of ultrafine particles of Fenofibrate in aqueous suspensions produced by sonoprecipitation. Powder Technol. 2020;363:310–25.
68. Kim DC, Yeo S Do. Habit modification of tamoxifen crystals using antisolvent crystallizations. Korean J Chem Eng. 2017;34:1466–74.
69. Kuk DH, Ha ES, Ha DH, Sim WY, Lee SK, Jeong JS, et al. Development of a resveratrol nanosuspension using the antisolvent precipitation method without solvent removal, based on a quality by design (QbD) approach. Pharmaceutics. 2019;11:688.
70. Afrose A, White ET, Howes T, George G, Rashid A, Rintoul L, et al. Preparation of ibuprofen microparticles by antisolvent precipitation crystallization technique: characterization, formulation, and in vitro performance. J Pharm Sci. 2018;107:3060–9.
71. Wada S, Kudo S, Takiyama H. Development of simultaneous control of polymorphism and morphology in indomethacin crystallization. J Cryst Growth. 2016;435:37–41.
72. Thorat AA, Dalvi SV. Ultrasound-assisted modulation of concomitant polymorphism of curcumin during liquid antisolvent precipitation. Ultrason Sonochem. 2016;30:35–43.
73. Mohapatra PK, Sireesha, Rathore V, Verma HC, Bibhuti, Rath P, et al. Fabrication and in vitro characterization of a novel nanosuspension of telmisartan: a poorly soluble drug prepared by antisolvent precipitation technique using 33 factorial design. Int J Appl Pharm. 2020;12:286–94.
74. Alshweiat A, Csóka IiI, Tömösi F, Janáky T, Kovács A, Gáspár R, et al. Nasal delivery of nanosuspension-based mucoadhesive formulation with improved bioavailability of loratadine: preparation, characterization, and in vivo evaluation. Int J Pharm. 2020;579:119166.
75. Aly UF, Sarhan HAM, Ali TFS, Sharkawy HAEB. Applying different techniques to improve the bioavailability of candesartan cilexetil antihypertensive drug. Drug Des Devel Ther. 2020;14:1851–65.
76. Li W, Zhao X, Sun X, Zu Y, Liu Y, Ge Y. Evaluation of antioxidant ability in vitro and bioavailability of trans -cinnamic acid nanoparticle by liquid antisolvent precipitate. J Nanomater. 2016;2016.
77. Bodnar K, Hudson SP, Rasmuson ÅC. Stepwise use of additives for improved control over formation & stability of mefenamic acid nanocrystals produced by antisolvent precipitation. Cryst Growth Des. 2017;17:454–66.
78. Tierney TB, Guo Y, Beloshapkin S, Rasmuson ÅC, Hudson SP. Investigation of the particle growth of fenofibrate following antisolvent precipitation and freeze-drying. Cryst Growth Des. 2015;15:5213–22.
79. Dalvi SV, Yadav MD. Effect of ultrasound and stabilizers on nucleation kinetics of curcumin during liquid antisolvent precipitation. Ultrason Sonochem. 2015;24:114–22.
80. Hao J, Gao Y, Zhao J, Zhang J, Li Q, Zhao Z, et al. Preparation and optimization of resveratrol nanosuspensions by antisolvent precipitation using box-behnken design. AAPS PharmSciTech. 2014;16:118–28.
81. Shariare MH, Altamimi MA, Marzan AL, Tabassum R, Jahan B, Reza HM, et al. In vitro dissolution and bioavailability study of furosemide nanosuspension prepared using design of experiment (DoE). Saudi Pharm J. 2019;27:96–105.
82. Rao Q, Qiu Z, Huang D, Lu T, Zhang ZJ, Luo D, et al. Enhancement of the apparent solubility and bioavailability of tadalafil nanoparticles via antisolvent precipitation. Eur J Pharm Sci. 2019;128:222–31.
83. Rahim H, Sadiq A, Khan S, Amin F, Ullah R, Shahat AA, et al. Fabrication and characterization of glimepiride nanosuspension by ultrasonication-assisted precipitation for improvement of oral bioavailability and in vitro α-glucosidase inhibition. Int J Nanomedicine. 2019;14:6287–96.
84. Wu M, Feng Z, Deng Y, Zhong C, Liu Y, Liu J, et al. Liquid antisolvent precipitation: an effective method for ocular targeting of lutein esters. Int J Nanomedicine. 2019;14:2667–81.
85. Hu TT, Zhao H, Jiang LC, Le Y, Chen JF, Yun J. Engineering pharmaceutical fine particles of budesonide for dry powder inhalation (DPI). Ind Eng Chem Res. 2008;47:9623–7.
86. Resende de Azevedo J. Ultrasound assisted crystallization of a new cardioactive prototype using ionic liquid as solvent. Ultrason Sonochem. 2019;55:32–43.
87. Prasad R, Panwar K, Katla J, Dalvi SV. Polymorphism and particle formation pathway of carbamazepine during sonoprecipitation from ionic liquid solutions. Cryst Growth Des. 2020;20:5169–83.
88. Grodowska K, Parczewski A. Organic solvents in the pharmaceutical industry. Acta Pol Pharm - Drug Res. 2010;67:3–12.
89. Resende de Azevedo J, Jean-Jacques L, Espitalier F, Ré MI. Solubility of a new cardioactive prototype drug in ionic liquids. J Chem Eng Data. 2014;59:1766–73.
90. Pedro SN, Freire CSR, Silvestre AJD, Freire MG. The role of ionic liquids in the pharmaceutical field: an overview of relevant applications. Int J Mol Sci. 2020;1–50.
91. Kunov-Kruse AJ, Weber CC, Rogers RD, Myerson AS. The a priori design and selection of ionic liquids as solvents for active pharmaceutical ingredients. Chem - A Eur J. 2017;23:5498–508.
92. Marrucho IM, Branco LC, Rebelo LPN. Ionic liquids in pharmaceutical applications. Annu Rev Chem Biomol Eng. 2014;5:527–46.
93. Adawiyah N, Moniruzzaman M, Hawatulaila S, Goto M. Ionic liquids as a potential tool for drug delivery systems. MedChemComm. 2016;7(10):1881–97. https://doi.org/10.1039/C6MD00358C.
94. Yang Q, Zu C, Li W, Wu W, Ge Y, Wang L, et al. Enhanced water solubility and oral bioavailability of paclitaxel crystal powders through an innovative antisolvent precipitation process: antisolvent crystallization using ionic liquids as solvent. Pharmaceutics. 2020;12:1–16.
95. An JH, Jin F, Kim HS, Ryu HC, Kim JS, Kim HM, et al. Investigation of the polymorphic transformation of the active pharmaceutical ingredient clopidogrel bisulfate using the ionic liquid AEImBF4. Cryst Growth Des. 2016;16:1829–36.
96. An JH, Kim WS. Antisolvent crystallization using ionic liquids as solvent and antisolvent for polymorphic design of active pharmaceutical ingredient. Cryst Growth Des. 2013;13:31–9.
97. Viçosa A, Letourneau JJ, Espitalier F, Inês Ré M. An innovative antisolvent precipitation process as a promising technique to prepare ultrafine rifampicin particles. J Cryst Growth. 2012;80–7.
98. Sahibzada MUK, Zahoor M, Sadiq A, ur Rehman F, Al-Mohaimeed AM, Shahid M, et al. Bioavailability and hepatoprotection enhancement of berberine and its nanoparticles prepared by liquid antisolvent method. Saudi J Biol Sci. 2021;28:327–32.
99. Gera S, Pooladanda V, Godugu C, Swamy Challa V, Wankar J, Dodoala S, et al. Rutin nanosuspension for potential management of osteoporosis: effect of particle size reduction on oral bioavailability, in vitro and in vivo activity. Pharm Dev Technol. 2020;25:971–88.

100. Wu W, Wang L, Wang L, Zu Y, Wang S, Liu P, et al. Preparation of honokiol nanoparticles by liquid antisolvent precipitation technique, characterization, pharmacokinetics, and evaluation of inhibitory effect on HepG2 cells. Int J Nanomedicine. 2018;13:5469–83.
101. Neerati P, Palle S. Resveratrol nanoparticle pretreatment improved the oral bioavailability of bromocriptine: involvement of liver and intestinal CYP3A enzyme inhibition. J Nat Sci Biol Med. 2019;10:209–16.
102. Wang Z, Zhao X, Zu Y, Wu W, Li Y, Guo Z, et al. Licorice flavonoids nanoparticles prepared by liquid antisolvent re-crystallization exhibit higher oral bioavailability and antioxidant activity in rat. J Funct Foods. 2019;57:190–201.
103. Wang L, Zhao X, Yang F, Wu W, Liu Y, Wang L, et al. Enhanced bioaccessibility in vitro and bioavailability of ginkgo biloba extract nanoparticles prepared by liquid anti-solvent precipitation. Int J Food Sci Technol. 2019;54:2266–76.
104. Sahibzada MUK, Sadiq A, Zahoor M, Naz S, Shahid M, Qureshi NA. Enhancement of bioavailability and hepatoprotection by silibinin through conversion to nanoparticles prepared by liquid antisolvent method. Arab J Chem. 2020;13:3682–9.
105. Som S, Singh SK, Khatik GL, Kapoor B, Gulati M, Kuppusamy G, et al. Quality by design-based crystallization of curcumin using liquid antisolvent precipitation: micromeritic, biopharmaceutical, and stability aspects. Assay Drug Dev Technol. 2020;18:11–33.
106. Zhao X, Wang W, Zu Y, Zhang Y, Li Y, Sun W, et al. Preparation and characterization of betulin nanoparticles for oral hypoglycemic drug by antisolvent precipitation. Drug Deliv. 2014;21:467–79.
107. Pandey KU, Dalvi SV. Understanding stability relationships among three curcumin polymorphs. Adv Powder Technol. 2019;30:266–76.
108. Wu W, Zu Y, Wang L, Wang L, Wang H, Li Y, et al. Preparation, characterization and antitumor activity evaluation of apigenin nanoparticles by the liquid antisolvent precipitation technique. Drug Deliv. 2017;24:1713–20.
109. Lei Y, Kong Y, Sui H, Feng J, Zhu R, Wang W. Enhanced oral bioavailability of glycyrrhetinic acid via nanocrystal formulation. Drug Deliv Transl Res. 2016;6:519–25.
110. Wu W, Zu Y, Wang L, Wang L, Li Y, Liu Y, et al. Preparation, characterization and antitumor activity evaluation of silibinin nanoparticles for oral delivery through liquid antisolvent precipitation. RSC Adv. 2017;7:54379–90.
111. Joye IJ, Davidov-Pardo G, McClements DJ. Encapsulation of resveratrol in biopolymer particles produced using liquid antisolvent precipitation. Part 2: stability and functionality. Food Hydrocoll. 2015;49:127–34.
112. Sun CC, Su H, Zheng GD, Wang WJ, Yuan E, Zhang QF. Fabrication and characterization of dihydromyricetin encapsulated zein-caseinate nanoparticles and its bioavailability in rat. Food Chem. 2020;330:127245.
113. Zheng D, Zhang QF. Bioavailability enhancement of astilbin in rats through zein− caseinate nanoparticles. J Agric Food Chem. 2019;67:5746–53.
114. Davidov-Pardo G, Joye IJ, McClements DJ. Encapsulation of resveratrol in biopolymer particles produced using liquid antisolvent precipitation. Part 1: preparation and characterization. Food Hydrocoll. 2015;45:309–16.
115. Zhang X, Zhang H, Xia X, Pu N, Yu Z, Nabih M, et al. Preparation and physicochemical characterization of soy isoflavone (SIF) nanoparticles by a liquid antisolvent precipitation method. Adv Powder Technol. 2019;30:1522–30.
116. Ramisetty KA, Pandit AB, Gogate PR. Ultrasound-assisted antisolvent crystallization of benzoic acid: effect of process variables supported by theoretical simulations. Ind Eng Chem Res. 2013;52:17573–82.
117. Lee SK, Sim WY, Ha ES, Park H, Kim JS, Jeong JS, et al. Solubility of bisacodyl in fourteen mono solvents and N-methyl-2-pyrrolidone + water mixed solvents at different temperatures, and its application for nanosuspension formation using liquid antisolvent precipitation. J Mol Liq. 2020;310.
118. Xia D, Cui F, Piao H, Cun D, Piao H, Jiang Y, et al. Effect of crystal size on the in vitro dissolution and oral absorption of nitrendipine in rats. Pharm Res. 2010;27:1965–76.
119. Meer TA, Sawant KP, Amin PD. Liquid antisolvent precipitation process for solubility modulation of bicalutamide. Acta Pharm. 2011;61:435–45.
120. Zu Y, Li N, Zhao X, Li Y, Ge Y, Wang W, et al. In vitro dissolution enhancement of micronized l-nimodipine by antisolvent re-crystallization from its crystal form H. Int J Pharm. 2014;464:1–9.
121. Deshpande RD, Gowda DV, Vegesna NSKV, Vaghela R, Kulkarni PK. The effect of nanonization on poorly water soluble glibenclamide using a liquid anti-solvent precipitation technique: aqueous solubility, in vitro and in vivo study. RSC Adv. 2015;5:81728–38.
122. Kim HJ, Yeo SD. Liquid antisolvent crystallization of griseofulvin from organic solutions. Chem Eng Res Des. 2015;97:68–76.
123. Matteucci ME, Hotze MA, Johnston KP, Williams RO. Drug nanoparticles by antisolvent precipitation: mixing energy versus surfactant stabilization. Langmuir. 2006;22:8951–9.
124. Zhang ZB, Shen ZG, Wang JX, Zhao H, Chen JF, Yun J. Nanonization of megestrol acetate by liquid precipitation. Ind Eng Chem Res. 2009;48:8493–9.
125. Zu Y, Sun W, Zhao X, Wang W, Li Y, Ge Y, et al. Preparation and characterization of amorphous amphotericin B nanoparticles for oral administration through liquid antisolvent precipitation. Eur J Pharm Sci. 2014;53:109–17.
126. Zhao H, Wang JX, Wang QA, Chen JF, Yun J. Controlled liquid antisolvent precipitation of hydrophobic pharmaceutical nanoparticles in a MicroChannel reactor. Ind Eng Chem Res. 2007;46:8229–35.
127. Zhang Z, Ji J. Large-scale preparation of stable irbesartan nanoparticles by high-gravity liquid antisolvent precipitation technique. Powder Technol. 2017;305:546–52.
128. Park SJ, Yeo SD. Liquid antisolvent recrystallization of phenylbutazone and the effect of process parameters. Sep Sci Technol. 2011;46:1273–9.
129. Joye IJ, Nelis VA, McClements DJ. Gliadin-based nanoparticles: fabrication and stability of food-grade colloidal delivery systems. Food Hydrocoll. 2015;44:86–93.
130. Kakran M, Sahoo NG, Tan IL, Li L. Preparation of nanoparticles of poorly water-soluble antioxidant curcumin by antisolvent precipitation methods. J Nanoparticle Res. 2012;14:1–11.
131. Rathod WR, Rathod VK. Continuous preparation of nimesulide nanoparticles by liquid antisolvent precipitation using spinning disc reactor. J Chem Technol Biotechnol. 2019;94:919–26.
132. Shah SR, Parikh RH, Chavda JR, Sheth NR. Application of Plackett-Burman screening design for preparing glibenclamide nanoparticles for dissolution enhancement. Powder Technol. 2013;235:405–11.
133. Mishra B, Sahoo J, Dixit PK. Enhanced bioavailability of cinnarizine nanosuspensions by particle size engineering: optimization and physicochemical investigations. Mater Sci Eng C. 2016;63:62–9.
134. Zhu WZ, Wang JX, Shao L, Zhang HX, Zhang QX, Chen JF. Liquid antisolvent preparation of amorphous cefuroxime axetil nanoparticles in a tube-in-tube microchannel reactor. Int J Pharm. 2010;395:260–5.
135. Roy S, Bachchhav SD, Mukhopadhyay M. Analysis of the mechanism of cholesterol particle formation by liquid antisolvent crystallization. Ind Eng Chem Res. 2021;60:7975–86.

136. Park SJ, Jeon SY, Yeo SD. Recrystallization of a pharmaceutical compound using liquid and supercritical antisolvents. Ind Eng Chem Res. 2006;45:2287–93.
137. Chen J, Sarma B, Evans JMB, Myerson AS. Pharmaceutical crystallization. Cryst Growth Des. 2011;11:887–95.
138. Leuenberger H. New trends in the production of pharmaceutical granules: batch versus continuous processing. Eur J Pharm Biopharm. 2001;289–96.
139. Benitez-Chapa AG, Nigam KDP, Alvarez AJ. Process intensification of continuous antisolvent crystallization using a coiled flow inverter. Ind Eng Chem Res. 2020;59:3934–42.
140. Wang J, Lakerveld R. Integrated solvent and process design for continuous crystallization and solvent recycling using PC-SAFT. AIChE J. 2018;64:1205–16.
141. Orehek J, Češnovar M, Teslić D, Likozar B. Mechanistic crystal size distribution (CSD)-based modelling of continuous antisolvent crystallization of benzoic acid. Chem Eng Res Des. 2021;170:256–69.
142. Solymosi T, Angi R, Basa-Dénes O, Ránky S, Ötvös Z, Glavinas H, et al. Sirolimus formulation with improved pharmacokinetic properties produced by a continuous flow method. Eur J Pharm Biopharm. 2015;94:135–40.
143. Hussain MN, Jordens J, John JJ, Braeken L, Van Gerven T. Enhancing pharmaceutical crystallization in a flow crystallizer with ultrasound: Anti-solvent crystallization. Ultrason Sonochem. 2019;59:104743.
144. Vancleef A, Seurs S, Jordens J, Van Gerven T, Thomassen LCJ, Braeken L. Reducing the induction time using ultrasound and high-shear mixing in a continuous crystallization process. Curr Comput-Aided Drug Des. 2018;8:326.
145. Davey RJ, Back KR, Sullivan RA. Crystal nucleation from solutions - transition states, rate determining steps and complexity. Faraday Discuss. 2015;9–26.
146. Ferguson S, Morris G, Hao H, Barrett M, Glennon B. In-situ monitoring and characterization of plug flow crystallizers. Chem Eng Sci. 2012;77:105–11.
147. Azad MA, Knieke C, To D, Davé R. Preparation of concentrated stable fenofibrate suspensions via liquid antisolvent precipitation. Drug Dev Ind Pharm. 2014;40:1693–703.
148. Rahimi M, Valeh-e-Sheyda P, Parsamoghadam MA, Azimi N, Abidi H. LASP and Villermaux/Dushman protocols for mixing performance in microchannels: effect of geometry on micromixing characterization and size reduction. Chem Eng Process Process Intensif. 2014;85:178–86.
149. Valeh-e-Sheyda P, Rahimi M, Parsamoghadam A, Adibi H. Effect of microchannel confluence angles on size reduction of curcumin nano-suspension via liquid anti-solvent precipitation process. J Taiwan Inst Chem Eng. 2015;46:65–73.
150. Shrimal P, Jadeja G, Patel S. Microfluidics nanoprecipitation of telmisartan nanoparticles: effect of process and formulation parameters. Chem Pap. 2021;75:205–14.
151. Chen H, Zhang X, Cheng Y, Qian F. Preparation of smectic itraconazole nanoparticles with tunable periodic order using microfluidics-based anti-solvent precipitation. CrystEngComm. 2019;21:2362–72.
152. Le NHA, Van PH, Yu J, Chan HK, Neild A, Alan T. Acoustically enhanced microfluidic mixer to synthesize highly uniform nanodrugs without the addition of stabilizers. Int J Nanomed. 2018;13:1353–9.
153. Rahimi M, Valeh-e-Sheyda P, Zarghami R, Rashidi H. On the mixing characteristics of a poorly water soluble drug through microfluidic-assisted nanoprecipitation: experimental and numerical study. Can J Chem Eng. 2018;96:1098–108.
154. Hu J, Ng WK, Dong Y, Shen S, Tan RBH. Continuous and scalable process for water-redispersible nanoformulation of poorly aqueous soluble APIs by antisolvent precipitation and spray-drying. Int J Pharm. 2011;404:198–204.
155. Hu J, Dong Y, Ng WK, Pastorin G. Preparation of drug nanocrystals embedded in mannitol microcrystals via liquid antisolvent precipitation followed by immediate (on-line) spray drying. Adv Powder Technol. 2018;29:957–63.
156. Dong Y, Ng WK, Hu J, Shen S, Tan RBH. Clay as a matrix former for spray drying of drug nanosuspensions. Int J Pharm. 2014;465:83–9.
157. Gu C, Liu Z, Yuan X, Li W, Zu Y, Fu Y. Preparation of vitexin nanoparticles by combining the antisolvent precipitation and high pressure homogenization approaches followed by lyophilization for dissolution rate enhancement. Molecules. 2017;22:2038.
158. Zhang J, Lv H, Jiang K, Gao Y. Enhanced bioavailability after oral and pulmonary administration of baicalein nanocrystal. Int J Pharm. 2011;420:180–8.
159. Xu LM, Zhang QX, Zhou Y, Zhao H, Wang JX, Chen JF. Engineering drug ultrafine particles of beclomethasone dipropionate for dry powder inhalation. Int J Pharm. 2012;436:1–9.
160. Kumar S, Shen J, Burgess DJ. Nano-amorphous spray dried powder to improve oral bioavailability of itraconazole. J Control Release. 2014;192:95–102.
161. Ma Q, Sun H, Che E, Zheng X, Jiang T, Sun C, et al. Uniform nano-sized valsartan for dissolution and bioavailability enhancement: influence of particle size and crystalline state. Int J Pharm. 2013;441:75–81.
162. Zhong J, Shen Z, Yang Y, Chen J. Preparation and characterization of uniform nanosized cephradine by combination of reactive precipitation and liquid anti-solvent precipitation under high gravity environment. Int J Pharm. 2005;301:286–93.
163. Pandey NK, Singh SK, Gulati M, Kumar B, Kapoor B, Ghosh D, et al. Overcoming the dissolution rate, gastrointestinal permeability and oral bioavailability of glimepiride and simvastatin co-delivered in the form of nanosuspension and solid self-nanoemulsifying drug delivery system: a comparative study. J Drug Deliv Sci Technol. 2020;60:102083.
164. Mahesh KV, Singh SK, Gulati M. A comparative study of top-down and bottom-up approaches for the preparation of nanosuspensions of glipizide. Powder Technol. 2014;256:436–49.
165. Zhang H, Meng Y, Wang X, Dai W, Wang X, Zhang Q. Pharmaceutical and pharmacokinetic characteristics of different types of fenofibrate nanocrystals prepared by different bottom-up approaches. Drug Deliv. 2014;21:588–94.
166. Bolourchian N, Nili M, Foroutan SM, Mahboubi A, Nokhodchi A. The use of cooling and anti-solvent precipitation technique to tailor dissolution and physicochemical properties of meloxicam for better performance. J Drug Deliv Sci Technol. 2020;55:101485.
167. Yeo SD, Lee JC. Crystallization of sulfamethizole using the supercritical and liquid antisolvent processes. J Supercrit Fluids. 2004;30:315–23.
168. Wu W, Zu Y, Zhao X, Zhang X, Wang L, Li Y, et al. Solubility and dissolution rate improvement of the inclusion complex of apigenin with 2-hydroxypropyl-β-cyclodextrin prepared using the liquid antisolvent precipitation and solvent removal combination methods. Drug Dev Ind Pharm. 2017;43:1366–77.
169. Pandey KU, Joshi A, Dalvi SV. Evaluating the efficacy of different curcumin polymorphs in transdermal drug delivery. J Pharm Investig. 2021;51:75–84.
170. Kedia K, Wairkar S. Improved micromeritics, packing properties and compressibility of high dose drug, cycloserine, by spherical crystallization. Powder Technol. 2019;344:665–72.
171. Azad MA, Sievens-Figueroa L, Davé RN. Fast release of liquid antisolvent precipitated fenofibrate at high drug loading from biocompatible thin films. Adv Powder Technol. 2018;29:2907–19.
172. Chandra A, Chondkar AD, Shirodkar R, Lewis SA. Rapidly dissolving lacidipine nanoparticle strips for transbuccal administration. J Drug Deliv Sci Technol. 2018;47:259–67.

173. Beck C, Sievens-Figueroa L, Gärtner K, Jerez-Rozo JI, Romañach RJ, Bilgili E, et al. Effects of stabilizers on particle redispersion and dissolution from polymer strip films containing liquid antisolvent precipitated griseofulvin particles. Powder Technol. 2013;236:37–51.
174. Wu W, Wang L, Wang S. Amorphous silibinin nanoparticles loaded into porous starch to enhance remarkably its solubility and bioavailability in vivo. Colloids Surfaces B Biointerfaces. 2021;198:111474
175. Joye IJ, McClements DJ. Production of nanoparticles by anti-solvent precipitation for use in food systems. Trends Food Sci Technol. 2013:109–23.
176. Langer K, Balthasar S, Vogel V, Dinauer N, Von Briesen H, Schubert D. Optimization of the preparation process for human serum albumin (HSA) nanoparticles. Int J Pharm. 2003;257:169–80.
177. Khan SA, Schneider M. Improvement of nanoprecipitation technique for preparation of gelatin nanoparticles and potential macromolecular drug loading. Macromol Biosci. 2013;13:455–63.